

COMPUTATION OF *SH* SYNTHETIC SEISMOGRAMS ALONG HORIZONTAL AND VERTICAL PROFILES BY THE ALEKSEEV-MIKHAILENKO METHOD

L.J. PASCOE¹, F. HRON¹ AND P.F. DALEY¹

ABSTRACT

The computation of *SH* synthetic seismograms for an isotropic vertically inhomogeneous medium using a technique originally developed by Alekseev and Mikhailenko is presented. An explicit finite-difference solution for the elastodynamic wave equation describing the propagation of *SH*-waves is determined after the dimensionality of the wave equation is reduced through the use of a finite Hankel transform. Our formulae are presented in a form that is suitable for direct computer application. To facilitate the development of such a computer code the finite-difference integral-transform method is briefly reviewed and a stability criterion is determined. In addition, some practical guidelines, based on our experience with computer programs employing the Alekseev-Mikhailenko method (AMM), are presented. This is done in order to enhance the tutorial value of the paper which should be considered as an introduction to the AMM numerical technique, as it is becoming increasingly popular among practicing seismologists due to the availability of continuing advances in computer power. In our paper an *SH* point torque source and a horizontal point force, both located at the surface, are used for the computation of synthetic seismograms. The numerical models presented illustrate the nature of wave propagation for a particular model containing two thin low-velocity layers in a homogeneous half-space. Both horizontal traces and vertical traces (VSP) are computed for the model, and the applicability of the method, when compared to other alternative seismic modelling techniques, is examined.

1. INTRODUCTION

The Alekseev-Mikhailenko method (AMM) (Alekseev and Mikhailenko, 1980; Mikhailenko and Korneev, 1984; Mikhailenko, 1984, 1985) used in this paper is closely related to the first in a series of synthetic-seismogram techniques developed for the modelling of various types of geological structures. The method is a hybrid technique combining finite-difference methods with finite-integral-transform methods to obtain a solution of high numerical accuracy.

The algorithm described in the paper is for *SH*-waves propagating in a vertically inhomogeneous medium. The problem is reduced to a finite-difference problem in the

vertical spatial dimension and time by removing the radial coordinate, in a cylindrical coordinate system, through the use of a finite Hankel transform. A highly accurate numerical solution to the problem is provided with which other, faster but less accurate, ray methods may be compared. This is especially useful when trying to obtain approximate solutions in certain areas, such as in the vicinity of a caustic in a vertically inhomogeneous medium, or near a critical point in a plane-layered medium where the reflected and head waves interfere.

The method is usually faster than most difference programs in two spatial dimensions with the benefit that grid dispersion may be significantly reduced (to within 2 or 3 percent) by utilizing a band-limited source pulse and establishing the number of terms to adequately approximate the infinite series which comprises the inverse finite Hankel transform. In addition, out-of-plane spreading is always included which is not the case in most finite-difference schemes for two-dimensional geological models. The price paid for this is that lateral inhomogeneities cannot be introduced. Fortunately, more sophisticated AMM three-dimensional techniques have been developed for modelling laterally inhomogeneous structures and analyzing diffracted events (Mikhailenko and Korneev, 1984).

For reflection-type shooting, where source-receiver offsets are small, and in ascertaining a highly accurate vertical seismic profile (VSP) response, the method discussed in this paper is the most useful one we know of, at least in the initial modelling stages. It is becoming evident, as field techniques for the acquisition of VSP data improve, that borehole parameters are as important as the shooting pattern in the seismic response obtained (Balch and Lee, 1984). Therefore, because of the simplicity of the technique presented in this paper compared to others in the AMM class, it is the most likely initial candidate for the incorporation of the necessary correction terms to account for physical processes in the borehole which affect the seismic disturbance recorded there.

The AMM technique employed in this paper for the computation of *SH*-waves may also be applied to the

Manuscript received by the Editor October 28, 1986; revised manuscript received April 21, 1988.

¹Institute of Earth and Planetary Physics, Department of Physics, University of Alberta, Edmonton, Alberta T6G 2J1

This work was supported by the Natural Sciences and Engineering Research Council of Canada in the form of Strategic Grant G-1090.

numerical modelling of the more complicated P - SV -wave field, where both longitudinal and shear modes of wave propagation exist. Such an application of the AMM technique has already been presented by, among others, the authors of this paper (Pascoe et al., 1988). Since the mathematical description of the SH -wave field is simpler than that governing the P - SV problem, this paper can also serve as an introduction to the above-mentioned paper. This possibility, prompted by the constructive suggestions of the reviewers of the earlier paper, resulted in placing a greater emphasis in the present paper on the formal exposition of the theory and the practical computational guidelines useful in the efficient numerical implementation of the AMM technique.

2. THE ALEKSEEV-MIKHAILENKO METHOD (AMM)

The equation of motion for an SH -wave in cylindrical coordinates (r, ϕ, z) , due to a point torque source located at the origin in an isotropic vertically inhomogeneous half-space is (Aleksiev and Mikhailenko, 1980; Mikhailenko and Korneev, 1984):

$$\frac{\rho(z)}{\mu(z)} \frac{\partial^2 u}{\partial t^2} = \frac{\mu'(z)}{\mu(z)} \frac{\partial u}{\partial z} + \frac{\partial^2 u}{\partial z^2} + \frac{\partial^2 u}{\partial r^2} + \frac{1}{r} \frac{\partial u}{\partial r} - \frac{u}{r^2}. \quad (1)$$

The particle-displacement vector, $\bar{\mathbf{u}}(r, z)$, is equal to $u(r, z)\hat{\mathbf{e}}_\phi$, where $\hat{\mathbf{e}}_\phi$ is a unit vector perpendicular to the plane of incidence. The quantities $\rho(z)$ and $\mu(z)$ are the density and Lamé's coefficient, respectively. The shear-wave velocity $v(z)$ is related to $\mu(z)$ by $\mu(z) = \rho(z)v^2(z)$. The primes indicate differentiation with respect to z . Equation (1) is subject to the initial conditions

$$u|_{t=0} = \frac{\partial u}{\partial t}|_{t=0} = 0. \quad (2)$$

A torque source located on the surface at $(r, z) = (0, 0)$ imposes the boundary condition (Aleksiev and Mikhailenko, 1980):

$$\tau_{\phi z}|_{z=0} = -\frac{f(t)}{2\pi} \frac{d}{dr} \left[\frac{\delta(r)}{r} \right], \quad (3)$$

which is equivalent to

$$\frac{\partial u}{\partial z}|_{z=0} = -\frac{f(t)}{2\pi\mu_0} \frac{d}{dr} \left[\frac{\delta(r)}{r} \right], \quad (4)$$

with μ_0 being the value of Lamé's coefficient at the free surface and $f(t)$ being the time dependence of the source pulse which contains an appropriate multiplicative amplitude constant assuring maintenance of proper dimensionality. The problem under consideration is fully specified by equation (1) subject to the initial conditions (2) and the boundary condition (4).

The dimensionality of equation (1) may be reduced by applying a finite first-order Hankel transform (Sneddon, 1972) given by

$$S(k_i, z, t) = \int_0^a u(r, z, t) J_1(k_i r) r dr, \quad 0 < r < a, \quad (5)$$

the inverse of which is

$$u(r, z, t) = \frac{2}{a^2} \sum_{i=1}^{\infty} \frac{S(k_i, z, t) J_1(k_i r)}{[J_2(k_i a)]^2}. \quad (6)$$

The quantities k_i are the roots of the transcendental equation $J_1(k_i a) = 0$, where $r = a$ is the upper bound of the closed interval $[0, a]$.

In accordance with the basic properties of hyperbolic differential equations (e.g., Jeffreys and Jeffreys, 1972, p. 531), an additional constraint $u|_{r=a} = 0$ may be imposed on the solution of the equation of motion (1) without influencing the seismic response in the region of interest for a given finite time interval provided that a is large enough. This is due to the fact that the imposition of the boundary condition $u|_{r=a} = 0$ is equivalent to the introduction of a totally reflecting surface at $r = a$. Thus, if this reflecting surface is set far enough from the source, the seismic response, in the region where the receivers are located, will not be influenced by any spurious reflections from the fictitious interface at a within the specified time window.

Upon application of the Hankel transform the equation of motion has the form

$$\frac{\partial}{\partial z} \left[\mu(z) \frac{\partial S}{\partial z} \right] - k_i^2 \mu(z) S = \rho(z) \frac{\partial^2 S}{\partial t^2}, \quad \begin{matrix} t \geq 0 \\ z \geq 0 \end{matrix} \quad (1')$$

subject to the transformed initial conditions

$$S|_{t=0} = \frac{\partial S}{\partial t}|_{t=0} = 0, \quad (2')$$

and transformed boundary condition

$$\frac{\partial S}{\partial z}|_{z=0} = \frac{f(t)k_i}{4\pi\mu_0}. \quad (4')$$

In addition to the reflections from the fictitious interface at $r = a$, there is a need to minimize reflections from the lower grid boundary, whose depth must be finite when the problem is solved by numerical methods. This may be accomplished by having this boundary sufficiently deep so that the reflections from it do not influence the seismic record for the time window being considered, or by introducing a damping term $[\gamma(z)\partial u/\partial t]$ into the equation of motion. These spurious reflections remain but, because they are heavily damped, their amplitudes will be negligible. For this case, the equation of motion (1') becomes

$$\frac{\partial}{\partial z} \left[\mu(z) \frac{\partial S}{\partial z} \right] - k_i^2 \mu(z) S = \rho(z) \frac{\partial^2 S}{\partial t^2} + \gamma(z) \frac{\partial S}{\partial t} \quad (1'')$$

where $\gamma(z) = 0$ in the region of interest and increases linearly with depth over several wavelengths to the lower grid boundary. A third possibility of eliminating spurious reflections from the lower grid boundary is to incorporate into the solution an absorbing boundary at some depth z_B (Clayton and Engquist, 1977).

In what follows, equation (1''), where the damping term has been introduced, will be used to determine the SH displacement. The transformed problem [(1''), (2') and (4')] must be solved at a finite number of roots of the equation $J_1(k_i a) = 0$, and this is accomplished quite efficiently by employing an explicit finite-difference scheme. The spatial grid chosen must be sufficiently fine so as to minimize grid dispersion, which causes a delaying and broadening of the signal so that the pulse develops an oscillatory tail (Aleksiev and Mikhailenko, 1980). In the results presented in this paper about 40 grid points per wavelength were required to reproduce adequately the pulse employed.

The determination of a finite-difference analogue for equation (1'') is facilitated through the use of a relation given by Mitchell (1969, pp. 23-25), which has:

$$\frac{\partial}{\partial z} \left[\mu(z) \frac{\partial S}{\partial z} \right]_{z=z_m} = \frac{a_m S_{m-1}^j - (a_m + a_{m+1}) S_m^j + a_{m+1} S_{m+1}^j}{(\Delta z)^2} + O(\Delta z)^2 \quad (7)$$

where

$$a_m = \left[\Delta z \int_{z_{m-1}}^{z_m} \frac{dz}{\mu(z)} \right]^{-1} \quad (8)$$

and the indices j ($1 \leq j < J$) and m ($1 \leq m < M$) refer to time and space, respectively. The upper bounds J and M are related to the specified time interval, T , and the depth, Z , to the grid boundary by $J\Delta t = T$ and $M\Delta z = Z$. An explicit finite-difference analogue to (1'') is given by

$$\frac{a_m S_{m-1}^j - (a_m + a_{m+1}) S_m^j + a_{m+1} S_{m+1}^j}{(\Delta z)^2} - k_i^2 \mu_m S_m^j = \rho_m \frac{S_m^{j+1} - 2S_m^j + S_m^{j-1}}{(\Delta t)^2} + \gamma_m \frac{S_m^{j+1} - S_m^{j-1}}{2\Delta t} \quad (9)$$

In this form it is clear that one can solve explicitly for the unknown quantity S_m^{j+1} at time step $(j+1)$ in terms of known values of S_m at the previous time steps j and $(j-1)$, as the rewriting of equation (9) indicates:

$$\left[\frac{\rho_m}{(\Delta t)^2} + \frac{\gamma_m}{2\Delta t} \right] S_m^{j+1} = \frac{a_m S_{m-1}^j}{(\Delta z)^2} - \left[\frac{(a_m + a_{m+1})}{(\Delta z)^2} - \frac{2\rho_m}{(\Delta t)^2} + k_i^2 \mu_m \right] S_m^j + \frac{a_{m+1} S_{m+1}^j}{(\Delta z)^2} - \left[\frac{\rho_m}{(\Delta t)^2} - \frac{\gamma_m}{2\Delta t} \right] S_m^{j-1} \quad (10)$$

To implement the boundary condition at the free surface ($m = 0$), it is assumed that at the spatial grid points, 0, 1 and 2, the medium is homogeneous with $\gamma = 0$, $\mu = \mu_0$ and $v = v_0$ at these points. As a consequence, equation (10) is simplified considerably in that region. Upon the introduction of a centered difference analogue on the grid point $m = 0$ for the boundary condition (4') an expression for S_{-1}^j is obtained. Substituting this expression into equation (10) for $m = 0$ results in the following explicit analogue:

$$S_0^{j+1} = 2v_0^2 \left[\frac{(\Delta t)^2}{(\Delta z)^2} \right] S_0^j - \left[\frac{2v_0^2 (\Delta t)^2}{(\Delta z)^2} + k_i^2 v_0^2 (\Delta t)^2 - 2 \right] S_0^j - S_0^{j-1} - \frac{k_i f(t) (\Delta t)^2}{2\pi\mu_0 (\Delta z)} \quad (11)$$

The seismic source pulse $f(t)$ used in the computer programs was that of an exponentially damped sine function expressed as

$$f(t) = Q_0 \sin[\omega_0 (t - \tau)] \exp \left\{ - \left[\frac{\omega_0 (t - \tau)}{\sigma} \right]^2 \right\}, \quad -\tau < t < \tau \quad (12)$$

Here, ω_0 is the predominant angular frequency, σ a damping factor, 2τ the approximate width of the pulse and Q_0 an amplitude containing a proper dimensionality constant.

In order to determine the seismic response for $0 < t \leq T$, $0 \leq z < Z$ and $0 \leq r \leq a$, it is necessary to evaluate $S(k_i, z, t)$ for each root k_i over the z - t grid ($0 \leq m < M$, $0 < j < J$). The response at any given depth z and source-receiver distance r is found from the inverse finite transform given by the truncated series:

$$u(r, z, t) = \frac{2}{a^2} \sum_{i=1}^N \frac{S(k_i, z, t) J_1(k_i r)}{[J_1(k_i a)]^2} = \frac{2}{a^2} \sum_{i=1}^N \frac{S(k_i, z, t) J_1(k_i r)}{[J_0(k_i a)]^2} \quad (13)$$

in which the relation $J_2(k_i a) = J'_1(k_i a) = J_0(k_i a)$ (Abramowitz and Stegun, 1968, p. 361) has been used. In solving for $S(k_i, z, t)$, equations (10) and (11) are used in conjunction with the initial conditions, equation (2'). The error introduced by truncation of the series will be discussed shortly.

Although the finite-difference analogues and the formulae for the series which must be summed to perform the inverse finite Hankel transform from the domain of wavenumber, k , to that of the spatial dimension, r , are given by equations (10), (11) and (13), there are some practical questions which should be addressed before beginning any numerical implementations:

- (1) What should be the grid spacing in the vertical (z) direction?
- (2) How many terms are necessary to approximate adequately the infinite series in the inverse summation?

Regarding question (1), it is first convenient and probably more instructive to speak in terms of wavelengths (WL) rather than metres, and periods (T) instead of seconds. The predominant wavelength, λ_0 , will be defined by the relation $1/\lambda_0 = f_0/v$, where f_0 is the predominant frequency ($\omega_0 = 2\pi f_0$) of the source pulse and v is the minimum shear-wave velocity encountered in the model under consideration. All other spatial dimensions will be defined relative to the predominant wavelength. As an example, a model with a predominant frequency of 10 Hz and minimum shear-wave velocity of 2500 m/s, results in a predominant wavelength of $\lambda_0 = 250$ m. Thus, if the model consists of a 2000-m layer overlying a half-space, the layer would, by the definition given above, be 8.0 WL thick, even if the layer displayed a velocity variation in the interval between the free surface and the top of the half-space. Also, an offset of 4000 m would translate to an offset of 16.0 WL. This definition of the predominant wavelength is chosen to be mathematically convenient and may differ from a more practical "physical" wavelength of the seismic pulse inferred from field data.

Numerical experimentation was required to ascertain the optimum number of grid points per wavelength. Much of this work was done by Professor B.G. Mikhailenko and his associates by comparing exact solutions with results obtained using the method discussed in this paper. It was their finding that for most applications 40 grid points per wavelength provided a sufficient accuracy of within 2 or 3 percent of the maximum amplitude in the synthetic trace.

As a final note on this point, time will be referred to in terms of periods (T) rather than seconds. A period, like a wavelength, is defined in terms of the predominant frequency of the source pulse by the relation $T=1/f_0$.

The number of terms which must be considered in the inverse transform summation to approximate adequately the infinite series [question (2)] is discussed in the paper of Martynov and Mikhailenko (1984) and will be repeated here to keep this paper as self-contained as possible. As stated in the above-mentioned paper, the required

number of terms in the series summation is related to the smoothness and duration of the source pulse $f(t)$ in the time domain [equation (12)]. The reason for this is that these two properties have a direct effect on the width of the spectrum $F(\omega)$ in the frequency domain. $F(\omega)$ is the Fourier time transform of $f(t)$, which for equation (12) may be written analytically (apart from some multiplicative constant involving τ and Q_0) as:

$$F(\omega) = \frac{\pi^{1/2}}{i\omega_0} \exp\left[-\frac{\sigma^2}{4}(1 + \omega/\omega_0)^2\right] \sinh\left(\frac{\omega\sigma^2}{2\omega_0}\right). \quad (14)$$

The spatial frequency (horizontal wavenumber), k , in a cylindrical coordinate system is related to the angular frequency, ω , according to the following formula, $k = \omega/v$, where v is the shear-wave velocity. It is then a sufficient condition to approximate the infinite inverse summation series by a finite number of terms which may be determined by estimating an upper bound on ω , say ω_u , beyond which the spectrum $F(\omega)$ is essentially zero. After the determination of ω_u , the quantity k_u may be obtained from the above relation. In the source pulse under consideration, the maximum value of $F(\omega)$ occurs at $\omega = \omega_0$, at the predominant frequency. The width of $F(\omega)$ in the frequency domain, i.e., where $F(\omega)$ is large when compared with $F(\omega_0)$, depends on σ . The larger the value of σ , the narrower the spectrum in the frequency domain and the longer the pulse duration in the time domain. In the time domain the duration of the pulse is approximately σ/f_0 . In estimating, k_u as $k_u = \omega_u/v$, the velocity v is chosen to be the minimum shear-wave velocity encountered in the medium under consideration. With $k_i = \xi_i/a$, where the ξ_i are obtained from the relation $J_1(\xi_i) = 0$, the following holds:

$$k_u = \frac{\omega_u}{v} = \frac{\xi_u}{a} \quad (15)$$

or

$$\xi_u = \frac{a\omega_u}{v}. \quad (16)$$

From the above relation it can be seen that the number of terms which must be used in the inverse summation series increases linearly with a , and, as the spectral width decreases with increasing values of σ , this results in fewer terms being required to approximate the series. For the pulse used in this paper, with $\sigma = 4$: $\omega_u \approx 2\omega_0$. As $\lambda_0 = f_0/v$, where v is the minimum shear-wave velocity in the medium, equation (16) becomes:

$$\xi_u \approx 4\pi\alpha \quad (17)$$

where $\alpha = a/\lambda_0$ is a dimensionless quantity. For large values of i , $\xi_i \approx \pi i$ (Abramowitz and Stegun, 1968), so that $\xi_u \approx N\pi$ and consequently $N = 4\alpha$, N being the number of terms used in the inverse series to approximate the infinite series summation.

Because there is a possibility of unlimited amplification of errors by the finite-difference method for an arbitrary choice of Δz and Δt , the stability criterion for the technique must be determined. The von Neumann condition for stability can be applied because of the separability of variables in the problem. In this method a harmonic decomposition of the error is made at grid points at a given time level. Following the procedure set out by Mitchell (1969, pp. 209-210), the inequality

$$v^2 \left(\frac{\Delta t}{\Delta z} \right)^2 + \frac{k_i^2}{4} v^2 (\Delta t)^2 < 1 \quad (18)$$

is obtained. This must be satisfied if the solution to the problem under consideration is to be stable. Since it is assumed that Δz has been chosen and the roots k_i and velocity v are known, the inequality (18) serves essentially for the determination of the time step Δt . It should be noted that v is the largest shear-wave velocity encountered on the grid.

3. NUMERICAL RESULTS

In order to obtain a necessary verification of the results produced by our programs with those presented in the literature, a particular model has been chosen for the case of *SH*-waves discussed in this paper. The model used in the computation of synthetic seismograms for a vertically inhomogeneous medium is that presented by Korn and Müller (1983) in which two thin low-velocity layers representing coal seams are embedded in a homogeneous half-space (Figure 1, Table 1). In their paper, *SH*-waves are generated by a horizontal point force at the surface and the results confirmed by comparison with the reflectivity method (Fuchs and Müller, 1971). Apart from a difference in the time dependence of the source pulses, the results obtained in this paper match those in Figure 2 of Korn and Müller, so that any further results obtained using the method described in the previous section were deemed to be accurate.

The synthetic seismograms due to a horizontal point force at the surface differ from those due to a torque source at the surface in that the dependence of the source-wavelet amplitude on the take-off angle of the ray at the source is removed. That is, if for a torque source the amplitude of a given ray is $u = A \sin \theta_0$ where θ_0 is the take-off angle of the ray at the surface, the amplitude for the same ray due to a horizontal point force substituted for the torque source is $u = A$ (Ben-Menahem and Singh, 1981).

The formal mathematical statement of the initial boundary-value problem for a horizontal point force is given in the Appendix for the sake of completeness. As the derivation of the finite-difference analogue and the implementation of the free-surface condition are essentially the same for both sources, only final formulae for this source type are presented in the Appendix. These for-

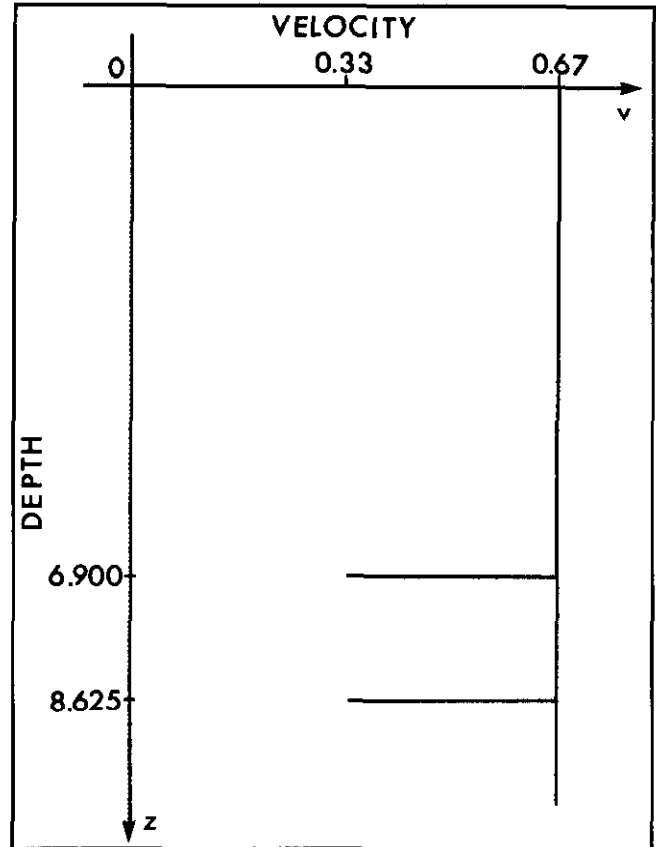


Fig. 1. Velocity-depth structure of the medium. Two coal seams with shear-wave velocities of 0.33 WL/T (866 m/s) and densities of $1.6 \times 10^3 \text{ kg/m}^3$ are set in a half-space whose velocity and density are 0.67 WL/T (1732 m/s) and $2.6 \times 10^3 \text{ kg/m}^3$, respectively. The depths of the coal seams are 6.90 WL (200 m) and 8.625 WL (250 m).

Layer	Velocity	Thickness	Density
1	1732 (0.67)	200 (6.900)	2.6×10^3
2	866 (0.33)	2 (0.300)	1.6×10^3
3	1732 (0.67)	50 (1.725)	2.6×10^3
4	866 (0.33)	2 (0.300)	1.6×10^3
Half-space	1732 (0.67)	—	2.6×10^3

Table 1. Parameters of the medium used in the computation of the synthetic seismograms in this paper; the unbracketed values (shear-wave velocity and thickness) are in m/s and m respectively while the bracketed values are in terms of wavelengths per period (WL/T) and wavelengths (WL). A wavelength is related to the shear-wave velocity of the medium in which the source is located and the predominant frequency of the source pulse. Hence, for a velocity of 1732 m/s and a predominant frequency of 60 Hz, as in the case here, 1 WL \approx 28.9 m. The density is given in kg/m^3 .

mulae are given a form that allows them to be programmed easily.

For the numerical calculations, the coal-seam model (Figure 1, Table 1) involves layers each 2 m thick having a density of $1.6 \times 10^3 \text{ kg/m}^3$ and a shear-wave velocity of 866 m/s embedded in a half-space of density $2.6 \times 10^3 \text{ kg/m}^3$ and a shear-wave velocity of 1732 m/s. The coal seams are placed at depths of 200 m and 250 m.

In order to match the arrivals given in the paper of Korn and Müller (1983), the predominant frequency of the time dependence of the force $f(t)$ was taken as 60 Hz rather than 30 Hz as stated there. In the seismograms presented here, source-receiver distances and depths are given in terms of wavelengths and time is given in terms of the predominant period. This arrangement makes it possible to give a much broader interpretation to any computed seismograms as the spatial dimensions of the medium and time scale in synthetic seismograms are directly linked to the parameters of wave propagation, i.e., to wavelength and period, respectively. With these changes the coal seams are at depths of 6.90 WL and 8.625 WL. One set of 10 receivers is located on the surface of the half-space at receiver intervals of 0.862 WL. The corresponding synthetic seismograms are shown in Figures 2 and 3. For the vertical seismic profiles another set of 24 receivers at equal depth increments of 0.375 WL has been placed at a horizontal distance of 4.31 WL from the source located on the surface. The related VSP seismograms are shown in Figures 5 and 6.

In a surface profile one expects to detect the direct ray, primary seam reflections, interseam multiples, and multiples between the surface and the seams. As expected, the direct arrival *A* as well as the primary reflections *B* and *C* are quite evident in Figure 2. In order to identify the remaining arrivals without destroying the relative ampli-

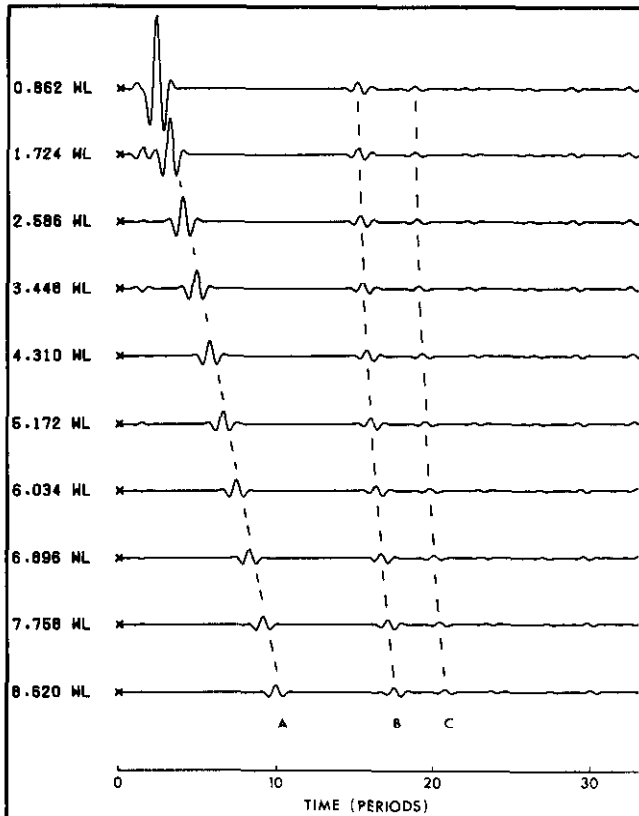


Fig. 2. Synthetic seismograms with receivers on the surface for a horizontal point force and the velocity-depth structure given in Table 1. *A* refers to the direct wave while *B* and *C* indicate the primary reflections from the two thin layers.

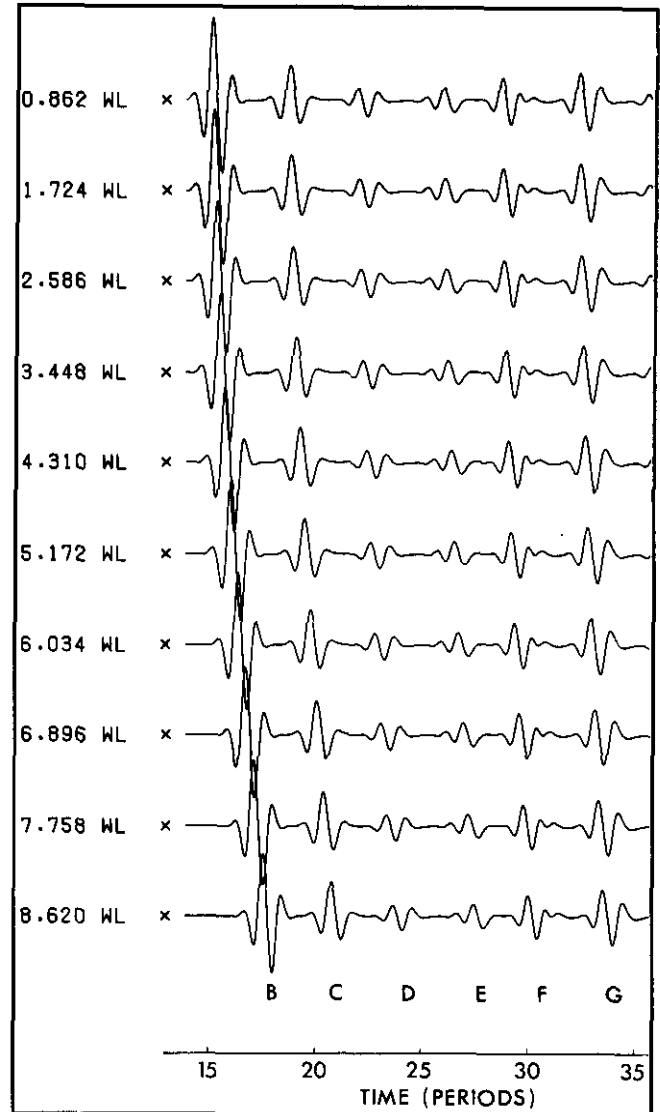


Fig. 3. The same surface traces as in Figure 2 with the direct arrival removed so that other arrivals which have undergone multiple reflections are enhanced. Identification of phases based on traveltimes is as follows:

$$B - S_1^2, C - S_1^2 S_2^2,$$

$$D - S_1^2 S_2^4, E - S_1^2 S_2^6, F - S_1^4, G - S_1^4 S_2^2$$

The subscripts on *S* indicate the layer of the ray segment while the superscript indicates the number of segments in the layers.

tude relation, the direct ray has been windowed out and the later arrivals amplified by decreasing the scale as shown in Figure 3. The primary reflections *B* and *C*, interseam multiples *D* and *E*, and the secondary reflections *F* and *G* have been identified and confirmed by matching traveltimes using standard ray methods.

There is a noticeable distortion of the original pulse shape in the primary reflections and later arrivals. This is due to the complex interference phenomena present in the wavelets which are reflected from, or transmitted

through, the very thin layers which represent the coal seams.

Only the windowed (direct arrival removed) surface traces are presented in Figure 4 for the case of an *SH* torque source. The significant difference between these arrivals and those for the horizontal point force is the amplitude dependence of the arrival on the take-off angle θ_0 made by the ray with the *z*-axis. As previously mentioned, Ben-Menahem and Singh (1981) showed that the amplitude of the disturbance is directly proportional to $\sin \theta_0$ for a point torque source, which is easily seen in the figure.

From the vertical profiles given in Figures 5 and 6, the nature of the wave propagation is immediately evident. Energy may arrive at a particular depth either from above or below. As seen in Figures 5 and 6, the direct arrival *A* represents the downgoing wave field, whereas arrivals *B* and *C* are reflections from each of the seams and represent upward-travelling disturbances. The interseam multi-

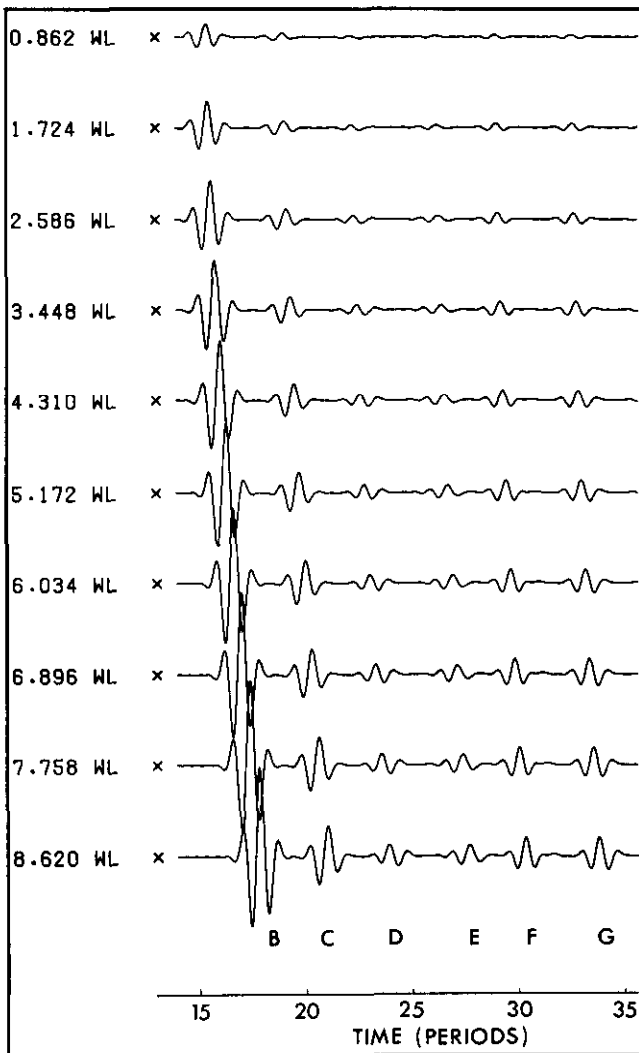


Fig. 4. Seismic traces with receivers located on the surface due to the torque source for the same coal model (Table 1) and the same offsets as were used in Figures 2 and 3. The direct arrival has been removed and the identification of phases is the same as that given in the caption of Figure 3.

ples are a result of the reflection labelled *D*. The primary reflection *B* from the uppermost coal seam is reflected once again at the free surface and propagates downward into the half-space as arrival *H*. The ease with which the nature of each event is visually determined in any set of seismograms along vertical profiles demonstrates how invaluable the VSP seismograms are in the interpretation of seismic traces recorded on the surface, as the commonly used traveltimes curves are frequently misleading and inconclusive, especially in more complex geological structures.

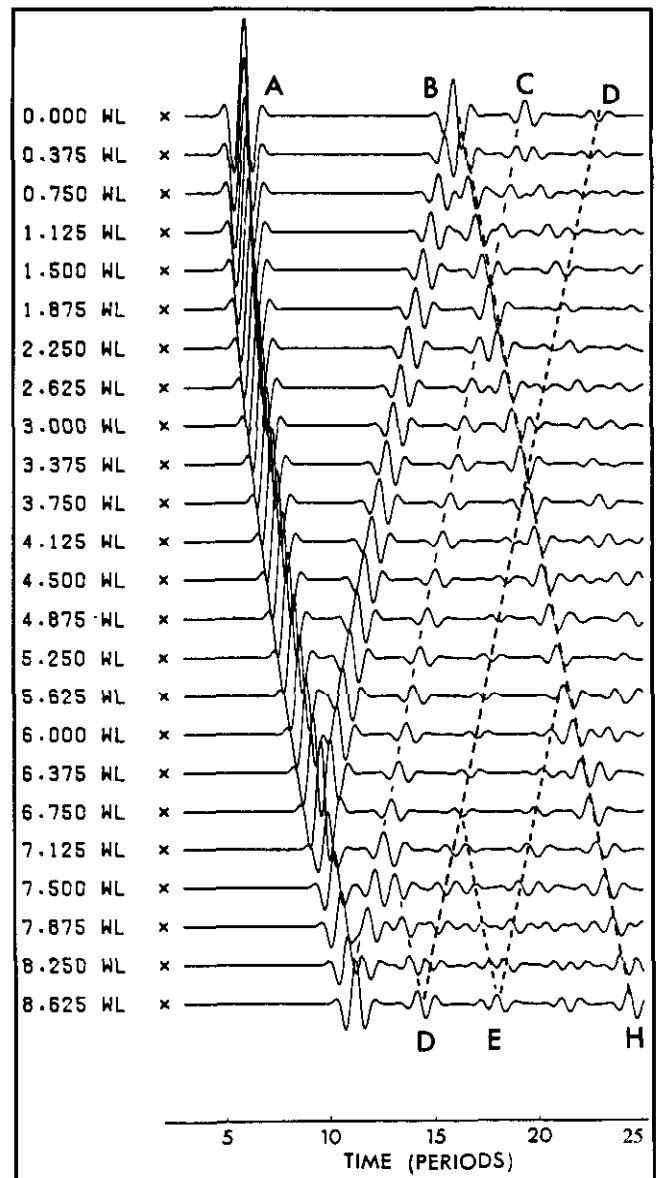


Fig. 5. Synthetic seismograms due to a horizontal point-force source computed for a vertical profile at the source-receiver distance of $r = 4.1$ WL in the coal-seam model (Table 1). The nature of each event can be directly inferred from the seismograms and checked against a more detailed phase identification obtained by ray methods and schematically shown in Figure 7.

4. CONCLUSION

All the information necessary to develop a computer code for the computation of a total *SH*-wave field due to a point source located in a vertically inhomogeneous medium is presented. The resultant computer program can be used for the production of *SH* synthetic traces along horizontal or vertical profiles depending on the nature of the problem under investigation. We used the Alekseev-Mikhailenko method for the development of theoretical formulae for horizontal point-force and torque-type sources. Advantages of the method were discussed in the text and demonstrated on the seismic traces presented in the paper. Included in the computed traces is the total wave field in which some distinct arrivals such as reflections, multiples, and surface waves are easily recognized. An additional advantage is the high numerical accuracy provided through the use of Hankel transforms in

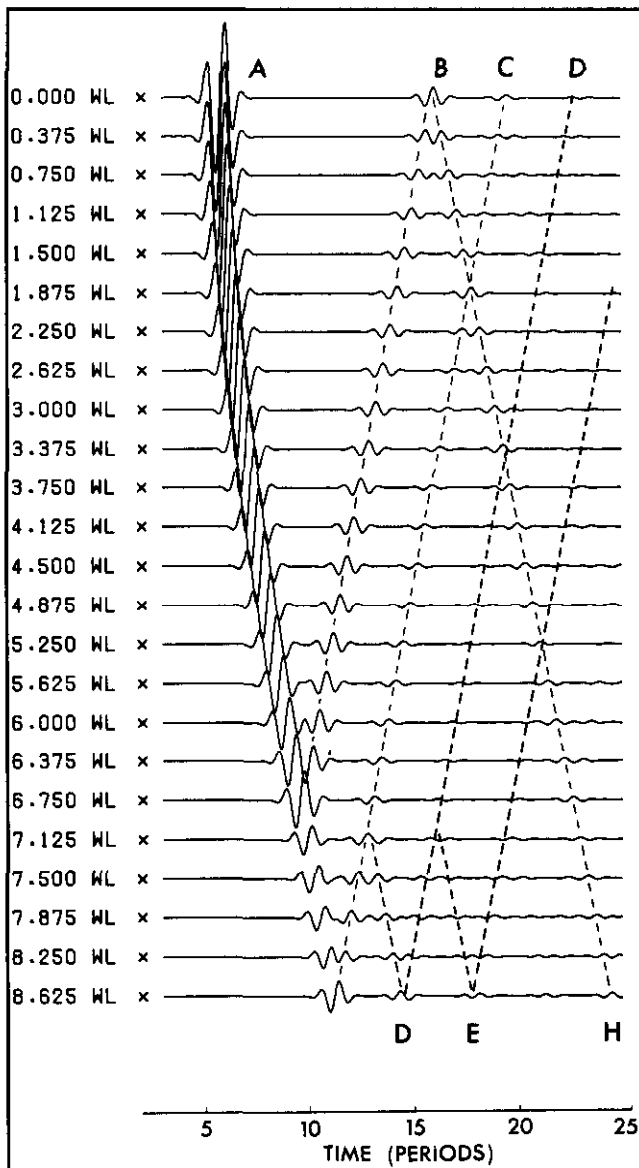


Fig. 6. A torque source equivalent of the VSP in Figure 5; see Figure 7 for identification of the individual arrivals.

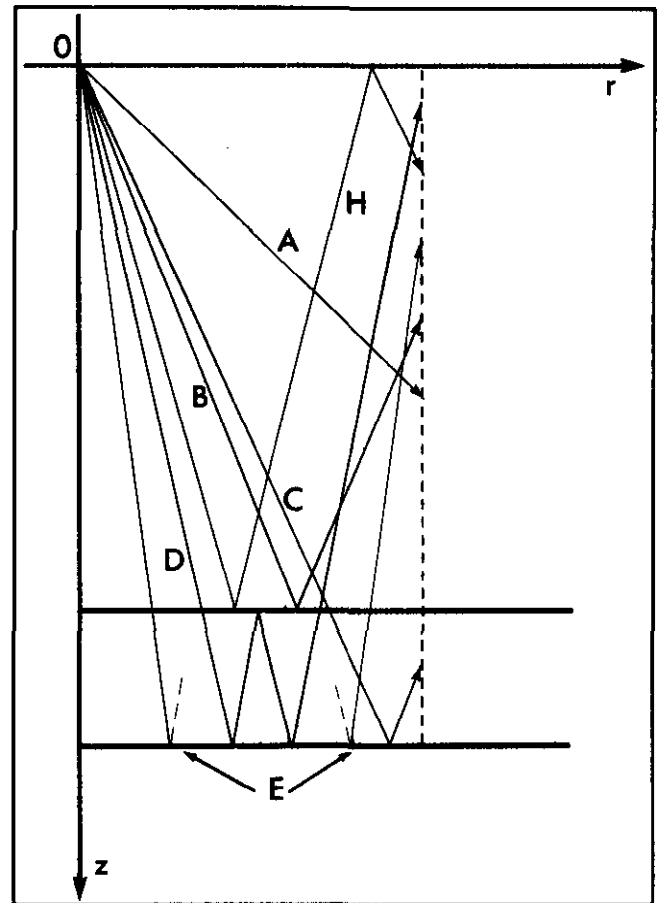


Fig. 7. A schematic of the rays which contribute to the VSP seismograms shown in Figures 5 and 6; these arrivals were determined from traveltimes computed using ray-tracing methods.

reducing the dimensionality of the wave equation, thereby limiting grid dispersion. The application of this numerical method to vertical seismic profile studies was also demonstrated. Unless the VSP seismograms are used, some ray methods must still be employed to identify particular arrivals seen in the horizontal profiles, and as mentioned in the Introduction, some form of correction term for borehole parameters should be introduced to obtain a more accurate synthetic.

REFERENCES

- Abramowitz, M. and Stegun, I.A., 1968, Handbook of mathematical functions: Dover Publ. Inc.
- Alekseev, A.S. and Mikhailenko, B.G., 1980, The solution of dynamic problems of elastic wave propagation in inhomogeneous media by a combination of partial separation of variables and finite-difference methods: *J. Geophys.* **48**, 161-172.
- Balch, A.H. and Lee, M.W., Eds., 1984, Vertical seismic profiling: Internat. Human Res. Dev. Corp.
- Ben-Menahem, A. and Singh, S.J., 1981, Seismic waves and sources: Springer-Verlag New York, Inc.
- Clayton, R. and Engquist, B., 1977, Absorbing boundary conditions for acoustic and elastic wave equations: *Bull. Seis. Soc. Am.* **67**, 1529-1540.
- Fuchs, K. and Müller, 1971, Computation of synthetic seismograms with the reflectivity method and comparison with observations:

Geophys. J. Roy. Astr. Soc. **23**, 417-433.

Jeffreys, H. and Jeffreys, B., 1972, *Methods of mathematical physics*, Cambridge Univ. Press.

Korn, M. and Müller, G. 1983, Comparison of the Alekseev-Mikhailenko method and the reflectivity method: Geophys. J. Roy. Astr. Soc. **72**, 541-556.

Martynov, V.N. and Mikhailenko, B.G., 1984, Numerical modelling of propagation of elastic waves in anisotropic inhomogeneous media for the halfspace and the sphere: Geophys. J. Roy. Astr. Soc. **76**, 53-63.

Mikhailenko, B.G., 1984, Synthetic seismograms for complex three-dimensional geometries using an analytical-numerical algorithm: Geophys. J. Roy. Astr. Soc. **79**, 963-986.

_____, 1985, Numerical experiment in seismic investigations: J. Geophys. **58**, 101-124.

_____, and Korneev, V.I., 1984, Calculation of synthetic seismograms for complex subsurface geometries by a combination of finite integral Fourier transforms and finite difference techniques: J. Geophys. **54**, 195-206.

Mitchell, A.R., 1969, *Computational methods in partial differential equations*: John Wiley & Sons, Inc.

Pascoe, L.J., Hron, F. and Daley, P.F., 1988, The Alekseev-Mikhailenko method applied to P-SV wave propagation in an elastic medium: Can. J. Earth Sci. **25**, 226-234.

Sneddon, I., 1972, *The use of integral transforms*: McGraw-Hill Book Co.

APPENDIX

The mathematical statement of the horizontal point force initial-boundary-value problem in a medium with azimuthal symmetry is formally given as

$$\rho \frac{\partial^2 u}{\partial t^2} = \mu \left[\frac{\partial^2 u}{\partial r^2} + \frac{1}{r} \frac{\partial u}{\partial r} \right] + \frac{\partial}{\partial z} \left(\mu \frac{\partial u}{\partial z} \right), \quad (\text{A1})$$

with the boundary condition

$$\left. \frac{\partial u}{\partial z} \right|_{z=0} = \left. \frac{\delta(r)}{2\pi r \mu_0} \right|_{r=0} f(t), \quad (\text{A2})$$

and the initial conditions

$$u \Big|_{t=0} = \left. \frac{\partial u}{\partial t} \right|_{t=0} = 0. \quad (\text{A3})$$

The pertinent finite Hankel forward and inverse pair used in reducing the dimensionality of the problem is given by

$$S(k_i, z, t) = \int_0^a u(r, z, t) J_0(k_i r) r dr \quad (\text{A4})$$

$$u(r, z, t) = \frac{2}{a^2} \sum_{i=1}^{\infty} \frac{S(k_i, z, t) J_0(k_i r)}{[J_1(k_i a)]^2} \quad (\text{A5})$$

as opposed to (5) and (6) which are valid for the torque source. The quantities k_i in this case are the roots of the equation $J_0(k_i a) = 0$.

Introducing the damping factor, Υ , to remove reflections from the lower grid boundary as in the torque-source case, and introducing the finite-difference analogues for the partial second-order derivatives in z and t , results in:

$$\begin{aligned} \left[\frac{\rho_m}{(\Delta t)^2} + \frac{\Upsilon_m}{2\Delta t} \right] S_m^{j+1} &= \frac{a_m S_{m-1}^j}{(\Delta z)^2} - \\ \left[\frac{(a_m + a_{m+1})}{(\Delta z)^2} - \frac{2\rho_m}{(\Delta t)^2} + m_i^2 \mu_m \right] S_m^j &+ \frac{a_{m+1} S_{m+1}^j}{(\Delta z)^2} \\ &= \left[\frac{\rho_m}{(\Delta t)^2} - \frac{\Upsilon_m}{2\Delta t} \right] S_m^{j-1} \end{aligned} \quad (\text{A6})$$

for $m > 0$, and

$$\begin{aligned} S_0^{j+1} &= 2v_0^2 \left[\frac{(\Delta t)^2}{(\Delta z)^2} \right] S_0^j - \\ &\left[\frac{2v_0^2 (\Delta t)^2}{(\Delta z)^2} + k_i^2 v_0^2 (\Delta t)^2 - 2 \right] S_0^j \\ &- S_0^{j-1} - \frac{f(t) (\Delta t)^2}{4\pi \mu_0 (\Delta z)} \end{aligned} \quad (\text{A7})$$

for $m = 0$. The definitions of a_m are given in the text, as are the stability criterion and method of determining the number of terms which must be considered to approximate adequately the inverse finite Hankel transforms.